Three-Dimensional Numerical Analysis of Ion Diamagnetic Effects on Interchange Mode in Heliotron Plasmas*)

Timothee NICOLAS[1)], Katsuji ICHIGUCHI[1,2)], Masahiko SATO[1)], Yasushi TODO[1,2)], Yasuhiro SUZUKI[1,2)], Akihiro ISHIZAWA[1,2)] and Satoru SAKAKIBARA[1,2)]

[1)]*National Institute for Fusion Science, 322-6 Oroshi-cho, Toki 509-5292, Japan*
[2)]*The Graduate University of Advanced Study, SOKENDAI, Toki 509-5292, Japan*

(Received 25 November 2014 / Accepted 28 January 2015)

The influence of the ion diamagnetic flow on the resistive interchange mode including dissipation in the Large Helical Device (LHD) plasmas is investigated with three-dimensional (3D) magnetohydrodynamic (MHD) codes. The contribution on the interchange mode stability depends on the difference between the ideal growth rate γ_{I} and the single fluid growth rate including resistivity and dissipation γ_{D}. When γ_{D} is close to γ_{I}, the ion diamagnetic effects are stabilizing. In this case the stabilization can be approximated by an analytic formula by analogy with the case without dissipation. When γ_{D} is far from γ_{I} the ion diamagnetic effects are destabilizing.

Keywords: heliotron, Large Helical Device, magnetohydrodynamics, interchange mode, flow, two-fluid effect

DOI: 10.1585/pfr.10.3403018

1. Introduction

The MHD stability of heliotrons has not yet been fully understood. This stability against interchange modes, which are pressure driven modes, depends not only on the plasma β but also on the horizontal position of the vacuum magnetic axis R_{ax}. Increasing R_{ax} makes the plasma more stable, however for large R_{ax} the confinement of high energy particles, which is crucial in a burning fusion plasma, is degraded. Thus a trade-off is needed to obtain an optimum configuration with both good MHD stability and good particle confinement.

In LHD, the original standard value of R_{ax} is 3.75 m. It was determined based on the stability against ideal interchange modes. Recently, experiments have shown that even for smaller values, down to $R_{\mathrm{ax}} \sim 3.6$ m, where the mode was predicted to be more unstable, the machine can be operated safely up to $\langle\beta\rangle \sim 5\%$ without major MHD event [1]. Here $\langle\beta\rangle$ is the volume averaged ratio between kinetic and magnetic pressure.

This means that LHD plasmas are more stable than predicted by ideal MHD. Understanding this stability is of major importance for the prediction of the characteristics of future heliotron fusion reactors. Many factors can explain the improved stability. First whereas the growth rate of the ideal interchange mode increases with the toroidal mode number n, in the experiment, the interchange modes actually observed have small mode number [2]. This can be explained by the fact that dissipation, *i.e.* thermal conductivity and viscosity, damps the higher n modes. This improves the overall stability, however the dissipation coefficients required to stabilize the mode to the experimentally observed level are too high compared with the measured values of these coefficients [3].

An other well-known stabilizing effect is the plasma flow. In the heliotron case as in the case of tokamaks, the locking of a mode in the magnetic perturbations coming from misalignment of the coils or from perturbation coils causes the plasma flow to stop in the vicinity of the mode's resonant surface, allowing the mode amplitude to grow significantly [4]. This phenomenon can lead to the collapse of the discharge. The fact that the mode grows after the rotation has stopped is an experimental evidence of the stabilizing effect of plasma flows. Thus, a theoretical analysis including the flow is desirable. The flow consists of the $\boldsymbol{E} \times \boldsymbol{B}$, parallel, and diamagnetic flows. In this study, we focus on the influence of the ion diamagnetic flow on the interchange mode stability. We study the stability numerically by utilizing 3D equilibrium and dynamics codes.

The generation of a 3D heliotron equilibrium with toroidal flows is a difficult problem because of some stringent theoretical constraints [5, 6]. In particular, it is much more difficult than in the tokamak case because of the lack of axisymmetry, which means the flow is not free even in the toroidal direction. The effects of the diamagnetic flows are implemented, with no modification of the equilibrium in the dynamics calculation.

In section 2 the physical model and the numerical methods are presented, in section 3 the results of the diamagnetic effects on the interchange mode stability in an LHD configuration are detailed. A discussion and summary follows in section 4.

author's e-mail: timothee_nicolas@ms.nifs.ac.jp

*) This article is based on the presentation at the 24th International Toki Conference (ITC24).

2. Physical Model and Numerical Methods

The MHD stability is investigated using the MIPS code [7], which solves a set of extended MHD equations as an initial value problem. Thus the observed mode in the linear phase is the one with the largest growth rate. The extended MHD equations used here are very close to the two-fluid model of Hazeltine and Meiss [8]. The normalized equations for the plasma mass density ρ, velocity $\boldsymbol{v}$, pressure p and magnetic field $\boldsymbol{B}$ are as follows:

$$\frac{\partial \rho}{\partial t} + \nabla \cdot \left(\rho(\boldsymbol{v} + \delta_{\rm i}\boldsymbol{v}_{\rm i}^{\star})\right) = S_\rho + \nabla \cdot D_\perp \nabla \rho, \tag{1}$$

$$\rho\left(\frac{\partial \boldsymbol{v}}{\partial t} + \boldsymbol{v}\cdot\nabla\boldsymbol{v} + \delta_{\rm i}\boldsymbol{v}_{\rm i}^{\star}\cdot\nabla\boldsymbol{v}_\perp\right) = \boldsymbol{J}\times\boldsymbol{B} - \nabla p + \frac{4}{3}\nabla\left[\nu\rho\nabla\cdot\boldsymbol{v}\right] - \nabla\times\left[\nu\rho\nabla\times\boldsymbol{v}\right], \tag{2}$$

$$\frac{\partial p}{\partial t} + \nabla\cdot(p\boldsymbol{v}) + (\Gamma-1)p\nabla\cdot\boldsymbol{v} = S_p + \nabla\cdot\chi_\perp\nabla p, \tag{3}$$

$$\frac{\partial \boldsymbol{B}}{\partial t} = \nabla\times(\boldsymbol{v}\times\boldsymbol{B} - \eta\boldsymbol{J}). \tag{4}$$

In these equations, the variable $\boldsymbol{v} = \boldsymbol{E}\times\boldsymbol{B}/B^2 + v_\parallel\boldsymbol{B}/B$ represents the MHD velocity, and $\boldsymbol{v}_{\rm i}^{\star} = \boldsymbol{B}\times\nabla p_{\rm i}/(\rho B^2)$ is the normalized ion diamagnetic velocity. The quantitites $S_\rho = -\nabla\cdot D_\perp\nabla\rho_{\rm eq}$ and $S_p = -\nabla\cdot\chi_\perp\nabla p_{\rm eq}$ are the sources of density and pressure, where $\rho_{\rm eq}$ and $p_{\rm eq}$ are the equilibrium density and pressure respectively. The normalization is as follows: the magnetic field is normalized to the field magnitude on the magnetic axis B_0, the density to the density on the magnetic axis ρ_0, the velocity to the Alfvén velocity $V_{\rm A} = B_0/\sqrt{\mu_0\rho_0}$, and the pressure to $\rho_0 V_{\rm A}^2$. The time is normalized to the Alfvén time $\tau_{\rm A} = x_0/V_{\rm A}$, where x_0 is the distance normalization. In addition, $D_\perp, \chi_\perp, \nu$ and η are, respectively, the particle and heat diffusion coefficients, the viscosity and the resistivity. As a result of this normalization, all the diamagnetic terms are multiplied by the parameter $\delta_{\rm i} = 1/(\omega_{\rm ci}\tau_{\rm A}) = d_{\rm i}/x_0 = K/(x_0\sqrt{n_0})$, where $\omega_{\rm ci} = eB/m_{\rm i}$ is the cyclotron frequency, $d_{\rm i}$ the ion skin depth and $K = \sqrt{m_{\rm i}/(\mu_0 e^2)}$ is a constant.

As can be seen from the normalization considerations above, changing the parameter $\delta_{\rm i}$ amounts to change either the size of the machine or the density normalization. If the plasma size is fixed, we have simply $\delta_{\rm i} \propto n_0^{-1/2}$. Some values of $\delta_{\rm i}$ corresponding to LHD plasma densities are given in Table 1. In the range $10^{18} \le n_0 \le 10^{20}$ $({\rm m}^{-3})$, the parameter $\delta_{\rm i}$ is smaller than 1.

Equations (1-4) require several comments. The model of Hazeltine and Meiss includes the Hall term in the induction equation. Here we do not include this term. In a first time, we are interested only in the ion diamagnetic effect, the electron effects will be included in a future study. The expression of the ion diamagnetic term in the momentum equation is obtained using the gyroviscous cancelation [8, 9].

An other important missing element in the pressure equation is the parallel heat conductivity $\chi_\parallel$, which should be several orders of magnitude larger than $\chi_\perp$. We do not include this term to avoid numerical difficulties. Indeed, for numerical stability, this term has to be treated implicitely, which increases significantly the simulation time in the case of large ratios of $\chi_\parallel/\chi_\perp$. For instance, for $\chi_\parallel/\chi_\perp = 10^5$, the simulation time is increased by roughly a factor of 5. The effect of the parallel heat conductivity is particularly important in the nonlinear evolution, because in this case a significant flattening of the pressure profile can be observed. However, we focus on the linear phase in this study. We checked the effect on the linear growth rate, and found an increase of only 10% of the growth rate for $\chi_\parallel/\chi_\perp = 10^5$. Therefore, we do not include the parallel heat conductivity in the present study.

Table 1 Some values of $\delta_{\rm i}$ and the corresponding density normalization n_0.

n_0 $({\rm m}^{-3})$	1×10^{18}	1×10^{19}	1×10^{20}
$\delta_{\rm i}$	0.23	0.072	0.023

Equations (1-4) are solved on an (R, φ, Z) mesh which is cartesian in the poloidal plane (R, Z). The poloidal plane is divided into two regions, called the plasma region in the center and the vacuum region surrounding it. The plasma region is defined by a condition on the equilibrium pressure $p_{\rm eq}$: $(p_{\max} - p_{\rm eq})/(p_{\max} - p_{\min}) < 0.998$, where $p_{\max}$ and $p_{\min}$ are the maximum and minimum values of $p_{\rm eq}$. The values of the fields are all kept constant in the vacuum region, and thus the boundary between the plasma and vacuum regions acts as a fixed boundary condition on the calculation in the plasma region. This kind of boundary conditions is sufficient to simulate interchange type instabilities, since they are localized around the resonant surface located in the plasma region. The resolution of the grid used in this study is $128\times640\times128$. The code solves the equations by an explicit fourth-order Runge-Kutta integration. The spatial derivatives are obtained by fourth order finite differences and an upwind scheme is used for the stabilization of advection terms. The equilibrium is obtained from the HINT2 code [10]. This code is able to obtain the static 3D heliotron equilibrium without assuming the existence of nested flux surfaces. In the case considered here, the inward-shifted LHD configuration is employed. It is characterized by $R_{\rm ax} = 3.60\,{\rm m}$ and $\gamma_{\rm c} = (a_{\rm c}/R_{\rm c})(N/l) = 1.129$, where $N = 10$ is the toroidal periodicity of the helical field, and $l = 2$, $a_{\rm c}$, $R_{\rm c}$ are respectively the pole number, the minor radius and the major radius of the helical coils.

3. Diamagnetic Effects on the Interchange Mode Stability

The dissipation coefficients are set to $\nu = \chi_\perp = D_\perp = 10^{-6}$, $\eta = 10^{-7}$. With these values and the equilibrium pressure profile given as $p = p_0(1-s)(1-s^4)$ where s is the normalized toroidal flux, the interchange mode is un-

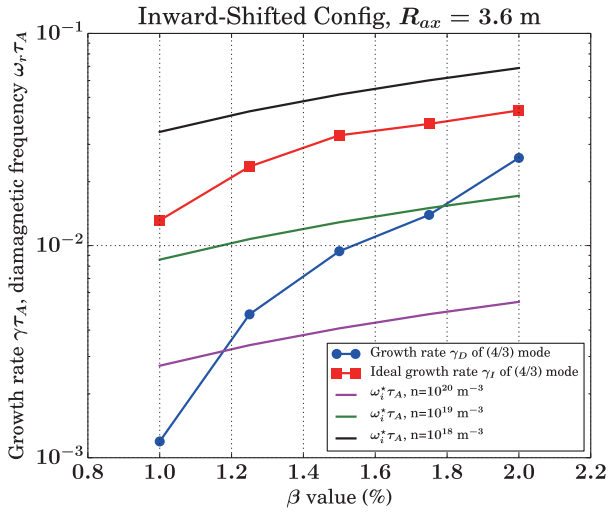

Fig. 1 Evolution of the single fluid growth rate γ_I and the diamagnetic frequency $\omega_i^\star$ of the 4/3 mode for different values of β. The evolution of γ_D with β is very strong.

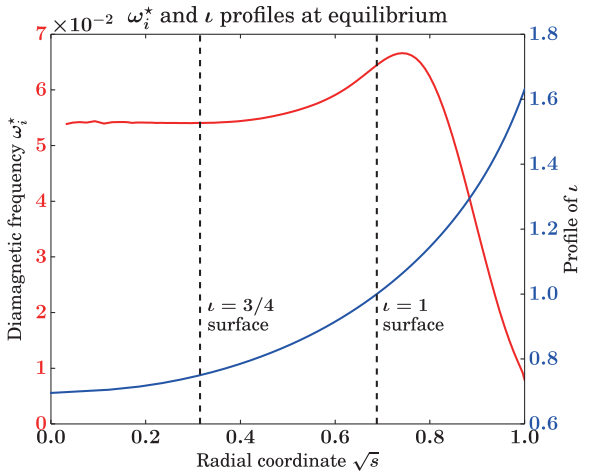

Fig. 2 Profile of $\omega_i^\star$ in the simulation, for the case $\delta_i = 0.228$ ($n_0 = 1 \times 10^{18}$ m^{-3}). The $\iota = 3/4$ and $\iota = 1$ surfaces are indicated by dashed vertical lines.

stable for $1\% \leq \beta \leq 2\%$, as shown in Fig. 1, where β represents the central β value. The most unstable mode is the $m/n = 4/3$ mode, where m and n are the poloidal and toroidal mode numbers. Figure 1 also shows the evolution with β of the single fluid growth rates γ_I (ideal) and γ_D (with dissipation) of the $m/n = 4/3$ interchange mode and the corresponding values of $\omega_i^\star$ for three different values of the density. It is seen that whereas $\omega_i^\star$ scales linearly with β, γ_D has a very strong dependence on β. From $\beta = 1\%$ to $\beta = 2\%$, there is an increase of a factor 20. If we look at the ratio between γ_D and γ_I, we have $\gamma_D/\gamma_I = 0.6$ for $\beta = 2\%$ and $\gamma_D/\gamma_I = 0.09$ for $\beta = 1\%$. Thus γ_D and γ_I can be considered close for $\beta = 2\%$ and very different for $\beta = 1\%$. This allows us to study two regimes: strong or weak modification of ideal stability by the dissipative effects. Each regime is examined in the density range 10^{18} m^{-3} to 10^{20} m^{-3}.

The effect of the diamagnetic flow can be decomposed in two contributions: (i) the shear of the flow and (ii) the modification of the dispersion relation. Sheared flows are able to stabilize large scale instabilities because they have a tendency to tear apart the structures. However, as shown in Fig. 2, the profile of the equilibrium diamagnetic frequency, $\omega_i^\star$, here defined on a constant s surface as

$$\omega_i^\star = \frac{2\pi m \delta_i}{\left(\oint \mathrm{d}l/|\boldsymbol{v}_{i,eq}^\star|\right)},$$

where $\mathrm{d}l$ is the length element on the curve of constant s, is virtually flat in the resonant region close to the $\iota = 3/4$ surface. Here, ι denotes the rotational transform. The shearing rate $\omega_s \equiv r\,\mathrm{d}\omega_i^\star/\mathrm{d}r < 10^{-4}$ is much too small to modify the stability of the mode, because $\omega_s \ll \gamma$ is easily verified in our simulations ($\gamma > 10^{-3}$ is the mode's growth rate).

Thus any effect of the diamagnetic flow comes directly from the modification of the dispersion relation due to the additional ion diamagnetic effects. Physically, the ion diamagnetic term modifies the inertia of the plasma, which modifies the energy balance and hence the stability of the interchange mode. The modification for ideal modes is given [11] by

$$\omega\left(\omega - \omega_i^\star\right) = -\gamma_I^2, \tag{5}$$

where γ_I is the growth rate of the ideal mode and ω is the complex eigenvalue of the mode including the ion diamagnetic effect. In principle according to Eq. (5), the mode is totally stabilized when $\omega_i^\star = 2\gamma_I$. In our simulations, the dissipation is also included so that Eq. (5) does not exactly hold. It is not trivial to understand how this relation is modified when dissipation is included. Thus, by analogy with Eq. (5), we consider a model dispersion relation

$$\omega\left(\omega - \omega_i^\star\right) = \Omega_D^2, \tag{6}$$

where $\Omega_D = \omega_D + i\gamma_D$ here is the single fluid complex frequency including dissipation (without the ion diamagnetic effects) of the dominant mode, and we will try to see if it is able to predict the stabilization of the interchange mode. Often $\omega_D = 0$ but since the force operator is Hermitian only in the ideal case, ω_D does not always vanish in the non-ideal case, as we will see later. If $\omega_D = 0$, equation (6) gives the expected diamagnetic stabilization and rotation frequency as

$$\gamma = \Im(\omega) = \gamma_D \sqrt{1 - \left(\omega_i^\star/2\gamma_D\right)^2}, \tag{7}$$

$$\omega_r = \Re(\omega) = \omega_i^\star/2. \tag{8}$$

Since the amplitude of $\omega_i^\star$ is fixed by the density, which often varies in the range $10^{18} - 10^{20}$ m^{-3} in the experiments, and the ideal growth rate is mainly determined by β, it is natural to explore the $(\omega_i^\star, \beta)$ parameter space.

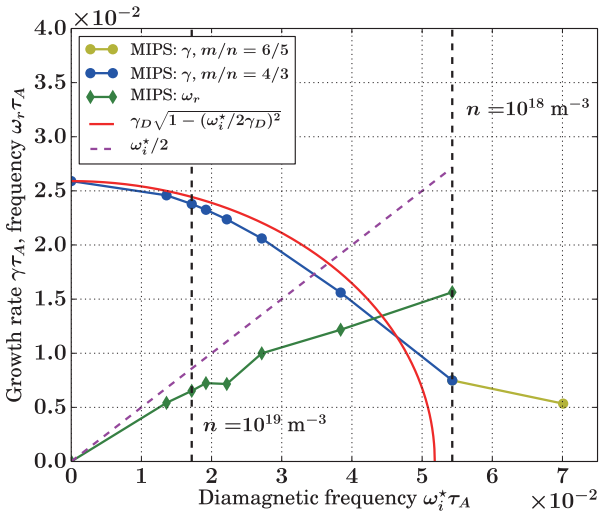

Fig. 3 Diamagnetic stabilization in the $\beta = 2\%$ case. The growth rate and frequency of the interchange mode are compared to those given by Eqs. (7-8). Rotation is in the ion direction. The vertical dashed lines indicate the correspondance between density and $\omega_i^\star$ for $n = 10^{18}$ and $n = 10^{19}$ m^{-3}.

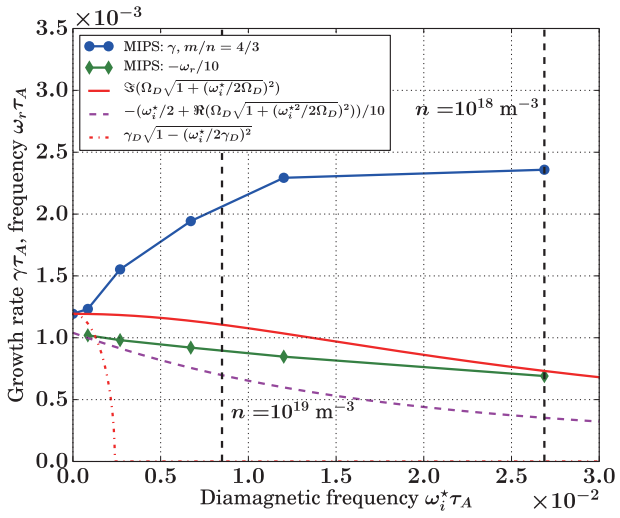

Fig. 4 Diamagnetic effects in the $\beta = 1\%$ case. The conventions are the same as in Fig. 3. To fit on the graph, the rotation frequency of the mode has been divided by -10. Rotation is in the electron direction.

The results are displayed in Fig. 3 and Fig. 4. The growth rate and frequency are plotted as the blue circles and the green diamonds respectively. Figure 3 shows the stabilization influence of $\omega_i^\star$ in the case where $\beta = 2\%$ and $\gamma_D/\gamma_I = 0.6$ ($\omega_D = 0$ in this case). The solid red and dashed magenta lines respectively show the growth rate and frequency γ and ω_r from Eqs. (7-8). In this case Eqs. (7-8) show good agreement with the numerical results until $\omega_i^\star \sim 1.5\gamma_D$ ($\omega_i^\star\tau_A = 4\times10^{-2}$). The mode rotates in the ion direction. For higher $\omega_i^\star$ the agreement is less good. The point $\omega_i^\star = 2.7\gamma_D$ ($\omega_i^\star\tau_A = 7\times10^{-2}$) is represented with a different color because the mode helicity is changed from $m/n = 4/3$ to $m/n = 6/5$. This does not indicate that the 4/3 mode is completely stabilized, but that the growth rate of the 4/3 mode was reduced below that of the 6/5 mode. Note that the 6/5 mode rotates in the electron direction.

Figure 4 shows the same study for the case where $\beta = 1\%$ and $\gamma_D/\gamma_I = 0.09$. Now the typical values of $\omega_i^\star$ become much larger than the single fluid growth rate. As can be seen in the figure, the growth rate increases with $\omega_i^\star$. This behavior is quite different from that in the $\beta = 2\%$ case, the mode is not stabilized at all. Contrary to the $\beta = 2\%$ case where the mode structure changes when $\omega_i^\star/\gamma_D$ is larger than 2, in the presently discussed $\beta = 1\%$ case, the 4/3 mode is still the dominant mode in the simulation even for $\omega_i^\star \gg 2\gamma_D$. The mode structure of the 4/3 mode is identical in the $\beta = 1\%$ and $\beta = 2\%$ cases, as seen by Fig. 5, which shows the pressure perturbation. The only small difference in the radial position of the mode can be attributed to the small difference of resonant surface position.

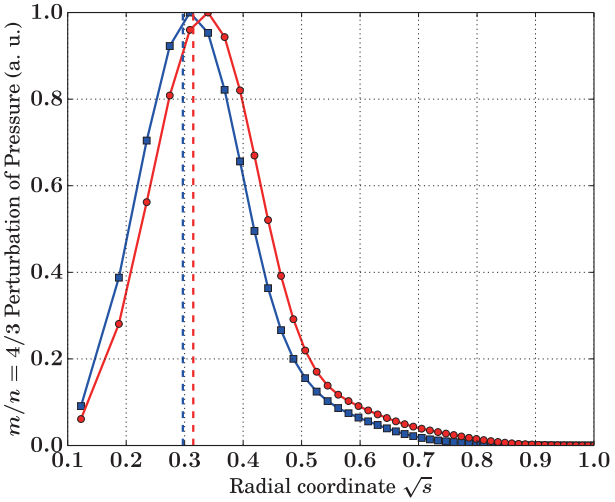

Fig. 5 Comparison of mode structure of $m/n = 4/3$ pressure perturbation for $\beta = 2\%$ and $\beta = 1\%$. In the $\beta = 2\%$ case, we have chosen $n = 2\times10^{18}$ m^{-3} ($\omega_i^\star\tau_A = 3.8\times10^{-2}$). In the $\beta = 1\%$ case, we have chosen $n = 5\times10^{18}$ m^{-3} ($\omega_i^\star\tau_A = 1.2\times10^{-2}$). The vertical dashed lines indicate the resonant surface position in the two cases.

The rotation of the 4/3 mode is in the electron diamagnetic direction, rather than in the ion diamagnetic direction. The frequency has a weak dependence on $\omega_i^\star$. On the figure, we have scaled it by a factor $-1/10$ in order to visualize it on the same graph. Note that the frequency does not go to zero for $\omega_i^\star = 0$, which reflects the fact that $\omega_D \neq 0$. Thus we are in a case where the single fluid problem contains complex eigenvalues. The interpretation is as follows. In the single fluid problem, there are two eigenvalues which are complex conjugate of each other, that is, they have same growth rate and opposite frequencies ω_D

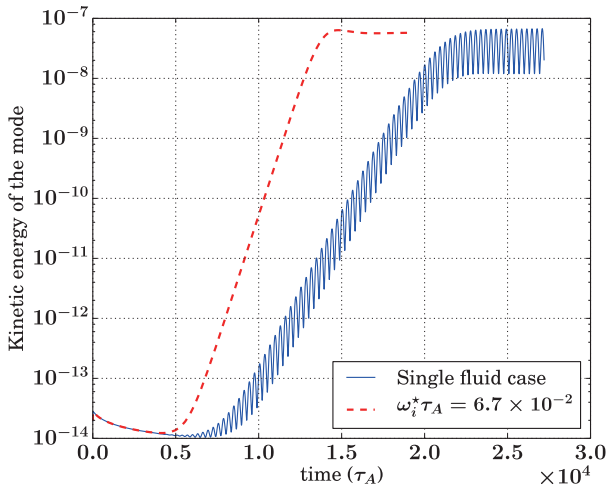

Fig. 6 Evolution of the mode energy in the single fluid case (blue line), and for $n = 1.6{\times}10^{19}$ m^{-3} ($\omega_i^\star \tau_A = 6.7{\times}10^{-2}$) (red dashed line). The first case displays a modulation corresponding to the existence of two eigenvalues with same growth rate and opposite frequency. The absence of modulation in the second case means that the degeneracy between the growth rates is removed by the diamagnetic effect. In this case, the mode with highest growth rate is the one which rotates in the electron direction.

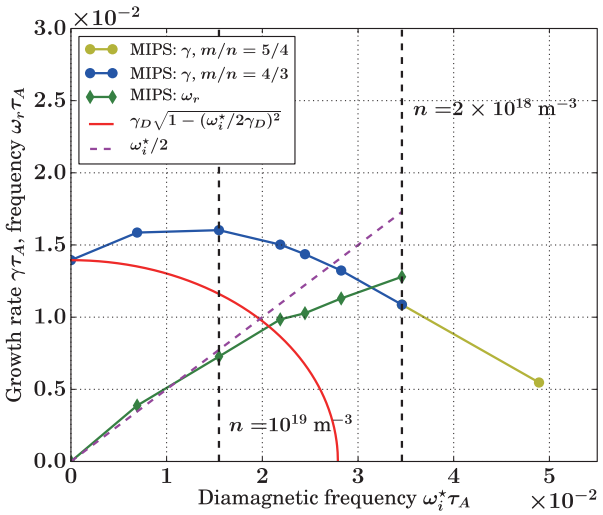

Fig. 7 Diamagnetic effects in the $\beta = 1.75\%$ case. The conventions are the same as in Fig. 3.

and $-\omega_D$. If the two solutions have comparable amplitude (which should be the case for random initial conditions), then the system does not rotate but we should observe a modulation of the mode energy at twice the frequency of the mode. We indeed observe such a modulation as shown in Fig. 6. From the period T of the oscillation, we can infer the absolute value of the pulsation in the single fluid case as $2\omega_D = 2\pi/T$, which gives $\omega_D\tau_A = 1.01 \times 10^{-2}$. Then when the diamagnetic frequency is included, the degeneracy in the growth rate between the two solutions is removed, so the modulation of the energy disappears (also shown in the figure). In this case we observe a rotation of the mode. When $\omega_i^\star$ tends to 0, the absolute value of this frequency should tend to the absolute value of the frequency of the single fluid case, ω_D. So by extrapolating the green curve to the vertical axis (and remembering the scaling by $-1/10$), we find the absolute value of ω_D to be $1.04 \times 10^{-2}\tau_A^{-1}$, in excellent agreement with the preceding estimate.

In this case where $\omega_D \neq 0$ we compare the results with the equivalent of Eqs. (7-8) in the general case:

$$\gamma = \Im\left(\Omega_D\sqrt{1+\left(\omega_i^\star/2\Omega_D\right)^2}\right), \tag{9}$$

$$\omega_r = \omega_i^\star/2 + \Re\left(\Omega_D\sqrt{1+\left(\omega_i^\star/2\Omega_D\right)^2}\right). \tag{10}$$

As can be seen in Fig. 4 where these two equations are plotted respectively as the red line and magenta dashed line, there is a qualitative agreement for the frequency: increasing the ion diamagnetic frequency causes a shift of the mode frequency toward the ion direction. However the model dispersion relation predicts stabilization even in this case, whereas the numerical result displays a clear destabilization. Note however that because $\omega_D \neq 0$, the stabilization predicted by Eqs. (9-10) is much weaker than if we had used Eqs. (7-8), in which case stabilization is predicted for $\omega_i^\star\tau_A = 2\gamma_D \sim 2.5 \times 10^{-2}$ (also represented in Fig. 4 as the dot-dashed red line).

We also examine the cases of $\beta = 1.75\%$, 1.5% and 1.25%, in which cases $\omega_D = 0$. The results show that the behaviour of the ion diamagnetic modification of the linear mode is gradually changed from $\beta = 2\%$ to $\beta = 1\%$. Figure 7 shows the $\beta = 1.75\%$ case. We can see that overall stabilization occurs toward large $\omega_i^\star$, and the rotation behaves according to $\omega_r = \omega_i^\star/2$, in the ion direction. However the growth rate increases and departs significantly from Eq. (7) for $\omega_i^\star\tau_A < 1.5 \times 10^{-2}$. This destabilization is checked from the numerical point of view. The resuts are recovered when increasing the poloidal resolution from 128×128 to 256×256. For larger ion diamagnetic frequency, $\omega_i^\star > 2\gamma_D$, the $m/n = 5/4$ mode takes over the 4/3 mode. This mode rotates in the electron direction.

4. Summary and Discussion

In this study, the dependence of the interchange mode on the ion diamagnetic flow is investigated. The results depend on the ratio between the growth rates with and without the dissipation γ_D/γ_I. When $\gamma_D/\gamma_I = 0.6$ the ion diamagnetic flow stabilizes the mode as in the case for the ideal mode. The growth rate decreases and the rotation frequency increases as $\omega_i^\star$ increases. The direction of the rotation is in the ion diamagnetic direction. These properties are due to the fact that the dissipation produces only a small change of the ideal mode. Therefore, the model equation Eq. (6) approximates the numerical results

well. For smaller values of γ_D/γ_I, destabilizing effects appear. The destabilization region where the growth rate increases with $\omega_i^\star$ extends as γ_D/γ_I decreases. In the case of $\gamma_D/\gamma_I = 0.09$, the growth rate increases with $\omega_i^\star$ for any value of $\omega_i^\star$. Furthermore, the mode rotates in the electron diamagnetic direction, with a frequency which tends to a finite value when $\omega_i^\star$ tends to zero, which means that the eigenvalue here is complex even in the single fluid situation. Even after taking this into account, the modification of the growth rate does not agree with the model dispersion relation. This shows that the dissipation affects significantly the dispersion relation of the mode in the presence of the diamagnetic effect. Therefore, Eq. (6) cannot recover the numerical results any more, and a more exact model is necessary to understand the observed behavior. The derivation of such a model is left as future work. The dispersion relation including both resistivity and the diamagnetic effect is given in [12] in the case of the internal kink mode, and such dispersion relation for the tearing mode based on the Glasser-Greene-Johnson method in tokamaks is discussed in [13]. Such formulation may help the derivation for the interchange mode in heliotrons.

Some problems remain unresolved in the present analysis. Firstly, the mode which appears after the reduction of the $m = 4$ mode growth rate, as $\omega_i^\star$ increases, has a poloidal mode number of $m = 5$ or 6. This fact is in apparent contradiction with the expectation that $\omega_i^\star$ has a stronger stabilizing effect for higher mode number, because $\omega_i^\star$ is proportional to m. Secondly, these higher modes rotate in the electron diamagnetic direction. This point is another problem. These problems should be treated in the future.

We have obtained a preliminary result of the nonlinear evolution of the plasma in the case of $\beta = 2\%$. In this case, the 5/4 mode becomes dominant after the 4/3 mode is saturated. The growth rate of the 5/4 mode is a little smaller than that of the 4/3 mode. During the growth of the 5/4 mode, the rotation direction reverses from the ion-diamagnetic direction to the electron diamagnetic direction. These properties show a similarity with the above linear analysis of the $\omega_i^\star$ dependence.

Regarding the understanding of the stability property of LHD plasmas in the viewpoint of the diamagnetic effects, the present study does not easily explain a significant stabilization. The ion diamagnetic effect contribution on the interchange mode is either stabilizing or destabilizing depending on γ_D/γ_I. However, this study remains limited because the vacuum configuration, the equilibrium condition and the dissipation parameters are kept fixed. Besides, some physical elements are neglected in the present formulation as discussed in Section 2. Therefore, in order to discuss the LHD stability comprehensively, we have to extend the range of parameters and the physical model in the numerical study.

Acknowledgments

One of the authors (T.N.) is an International Research Fellow of the Japan Society for the Promotion of Science. This work is supported by the budget NIFS14KNST063 of National Institute for Fusion Science, and JSPS KAKENHI Grant Number 26-04728 and Scientific Research (C) 22560822. Plasma simulator (NIFS) and Helios(IFERC-CSC) were utilized for the numerical calculations.

[1] H. Yamada *et al.*, Nucl. Fusion **51(9)**, 4021 (2011).
[2] Y. Takemura *et al.*, Plasma Fusion Res. **8**, 1402123 (2013).
[3] K. Ichiguchi, J. Plasma Fusion Res. SERIES **3**, 576 (2000).
[4] Y. Takemura *et al.*, Nucl. Fusion **52(10)**, 102001 (2012).
[5] A. Bondeson and R. Iacono, Phys. Fluids B **1(7)**, 1431 (1989).
[6] P. Helander *et al.*, Phys. Rev. Lett. **101(14)**, 145003 (2008).
[7] Y. Todo *et al.*, Plasma Fusion Res. **5**, S2062 (2010).
[8] R.D. Hazeltine *et al.*, *Plasma Confinement* (Dover Publications, Inc, Mineola (New York), 2003).
[9] J.J. Ramos, Phys. Plasmas **12**, 112301 (2005).
[10] Y. Suzuki *et al.*, Nucl. Fusion **46(11)**, L19 (2006).
[11] J. Connor *et al.*, Nucl. Fusion **24(8)**, 1023 (1984).
[12] G. Ara *et al.*, Ann. Phys. (N.Y.) **112(2)**, 443 (1978).
[13] D. Meshcheriakov *et al.*, Phys. Plasmas **19(9)**, 092509 (2012).